

Thermodynamics of the *bis*-(η^6 -*m*-xylene)molybdenum fulleride [[η^6 -(*m*-xylene) $_{2}$ Mo] $^{\bullet+}$ [C $_{60}$] $^{\bullet-}$]

A. V. Markin · V. A. Ruchenin · N. N. Smirnova ·
G. V. Markin · S. Yu. Ketkov · V. A. Kuropatov ·
V. K. Cherkasov · G. A. Abakumov · G. A. Domrachev

ESTAC2010 Conference Special Issue
© Akadémiai Kiadó, Budapest, Hungary 2010

Abstract In this study, the temperature dependence of heat capacity $C_p^\circ = f(T)$ of crystalline *bis*-(η^6 -*m*-xylene)-molybdenum fulleride between $T = (8 \text{ and } 320) \text{ K}$ was measured by precision adiabatic vacuum calorimetry. Also the temperature dependence of EPR signal parameters of *bis*-(η^6 -*m*-xylene)molybdenum fulleride in the range from 120 to 300 K was investigated by electron paramagnetic resonance. In the interval 175–220 K the reversible endothermic transformation was detected and its thermodynamic characteristics were estimated. This transformation was caused by the dissociation of the (C $_{60}^-$) $_2$ dimer in the [[η^6 -(*m*-xylene) $_{2}$ Mo] $^{\bullet+}$ [C $_{60}$] $^{\bullet-}$] fulleride during heating. Based on the experimental data, the standard ($p^\circ = 0.1 \text{ MPa}$) thermodynamic functions, namely, the heat capacity, enthalpy, entropy, and Gibbs function were calculated for dimeric fulleride in the interval from $T \rightarrow 0$ to 175 K as well as for monomeric [[η^6 -(*m*-xylene) $_{2}$ Mo] $^{\bullet+}$ [C $_{60}$] $^{\bullet-}$] complex between 220 and 320 K. The standard thermodynamic properties of tested fulleride and previously studied C $_{60}$ fullerite and neutral dimer (C $_{60}$) $_2$ were compared.

Keywords *Bis*-(η^6 -*m*-xylene)molybdenum fulleride · Adiabatic vacuum calorimetry · Heat capacity · Thermodynamic functions · Standard thermodynamic functions

A. V. Markin (✉) · V. A. Ruchenin · N. N. Smirnova
Chemistry Institute, Nizhny Novgorod State University, Gagarin
Pr. 23/5, 603950 Nizhny, Novgorod, Russian Federation
e-mail: markin@calorimetry-center.ru

G. V. Markin · S. Yu. Ketkov · V. A. Kuropatov ·
V. K. Cherkasov · G. A. Abakumov · G. A. Domrachev
Razuvaev Institute of Organometallic Chemistry of Russian
Academy of Sciences, Tropinin Str. 49, 603950 Nizhny,
Novgorod, Russian Federation

Introduction

The discovery of the method for producing C $_{60}$ fullerenes in macroquantities [1] has laid a new field of research. Thus, different properties of functional fullerene derivatives with valuable characteristics have been extensively investigated. The study of donor–acceptor complexes of fullerenes where the latter play the role of relatively strong acceptors is dictated by the search for new unique materials. Such materials exhibit interesting optical, electrical conductivity, and magnetic properties [2–10]. Most often, fullerene complexes with aromatic hydrocarbons as donor partners were synthesized and their properties were studied [2, 11–13].

As a result, on studying the thermal behavior of some *bis*-(η^6 -arene)chromium and *bis*-(η^6 -arene)molybdenum fullerides [12, 14–21], the low-temperature dimerization of anion-radicals of the fullerene at cooling was detected. The data about bonding strength between fullerene fragments in [Cr(Cp *) $_2$] $^+$ C $_{60}^-$ ·2C $_6$ H $_4$ Cl $_2$ complex are presented in Ref. [19] and its give a chance for comparison with dissociation energy of bond for the neutral dimer (C $_{60}$) $_2$ [22–24].

The calorimetric study of the reversible dimerization process of fullerene molecules in crystalline complexes was carried out for [[η^6 -C $_7$ H $_8$] $_2$ Cr] $^{\bullet+}$ [C $_{60}$] $^{\bullet-}$ [11], [[η^6 -Ph $_2$] $_2$ Cr] $^{\bullet+}$ [C $_{60}$] $^{\bullet-}$ [16], [[η^6 -*t*-BuPh] $_2$ Cr] $^{\bullet+}$ [C $_{60}$] $^{\bullet-}$ [17], and [[η^6 -EtOPh] $_2$ Cr] $^{\bullet+}$ [C $_{60}$] $^{\bullet-}$ [18].

There have been no data about heat capacity and thermodynamic properties of crystalline *bis*-(η^6 -*m*-xylene)-molybdenum fulleride in the literature. Those are, however, necessary as the fundamental data for new functional derivatives of C $_{60}$ and to understand the nature of low-temperature dimerization of fullerene fragments as well as to detect the influence of organoelement groups on the “hardness” and the stability of bound between fullerene

fragments in the low-temperature dimeric phase of $(C_{60}^-)_2$. With regard to the foregoing, the thermodynamic study of one of the representatives of *bis*-(η^6 -arene)molybdenum fullerides $[(\eta^6\text{-}(m\text{-xylene}))_2\text{Mo}]^{\bullet+}[\text{C}_{60}]^{\bullet-}$ is actual and urgent. The presence of the values of these functions at some temperature values will allow to estimate the possibility of different chemical processes with *bis*-(η^6 -*m*-xylene)molybdenum fulleride in defined conditions.

This study is a part of complex investigations of thermodynamic properties of C_{60} fullerides and describes the calorimetric investigation of heat capacity of the crystalline $[(\eta^6\text{-}(m\text{-xylene}))_2\text{Mo}]^{\bullet+}[\text{C}_{60}]^{\bullet-}$ in the range from 8 to 320 K, determination of the temperature interval of transformation that was caused by the dissociation of the $(C_{60}^-)_2$ dimer, and the formation of the $[(\eta^6\text{-}(m\text{-xylene}))_2\text{Mo}]^{\bullet+}[\text{C}_{60}]^{\bullet-}$ fulleride during heating, estimation of its standard thermodynamic characteristics; calculation of the standard ($p^\circ = 0.1$ MPa) thermodynamic functions heat capacity, enthalpy, entropy, and Gibbs function for fulleride dimer in the range from $T \rightarrow 0$ to 175 K and for $[(\eta^6\text{-}(m\text{-xylene}))_2\text{Mo}]^{\bullet+}[\text{C}_{60}]^{\bullet-}$ monomeric complex for the interval between 220 and 320 K; comparison the standard thermodynamic characteristics of the fulleride under study, of C_{60} fullerite and neutral dimer $(C_{60})_2$, as well as some previously studied fullerides.

Experimental

Sample

Bis-(η^6 -*m*-xylene)molybdenum fulleride $[(\eta^6\text{-}(m\text{-xylene}))_2\text{Mo}]^{\bullet+}[\text{C}_{60}]^{\bullet-}$ (gross formula $C_{76}H_{20}Mo$) was synthesized by the method described elsewhere [15]. The solution of $[(\eta^6\text{-}(m\text{-xylene}))_2\text{Mo}]^0$ in toluene was added to the saturated solution of C_{60} in toluene at room temperature. The resulting sediment was decanted and then washed by toluene and dried in vacuum. The elemental analysis yielded the Mo composition at 9.23% which compares with 9.34% calculated for $C_{76}H_{20}Mo$. The *m*-xylene and equimolar mixture of fullerene with molybdenum was quantitatively formed at thermo-decomposition.

The ion structure of fulleride was approved by results of ESR and electron spectra. The ESR spectra were recorded on Bruker EPX radiospectrometer and electron spectra—on PerkinElmer Lambda25 spectrometer. The EPR spectrum of *bis*-(η^6 -*m*-xylene)molybdenum fulleride in tetrahydrofuran (THF) at 293 K shows a line with typical for cation $[\text{Mo}(\eta^6\text{-arene})_2]^{\bullet+}$ hyperfine structure. Thus, *bis*-(η^6 -*m*-xylene)molybdenum is the cation-radical in fulleride. The visible spectroscopy of *bis*-(η^6 -*m*-xylene)molybdenum fulleride in THF has shown the presence of absorption band which is characteristic for $C_{60}^{\bullet-}$ at $\lambda = 1081$ nm. Thus,

bis-(η^6 -*m*-xylene)molybdenum fulleride is the ion-radical salt: $[(\eta^6\text{-}(m\text{-xylene}))_2\text{Mo}]^{\bullet+}[\text{C}_{60}]^{\bullet-}$.

The tested sample is relatively unstable in air, and therefore, all operations related to its preparation for calorimetric measurements were conducted in a chamber in a flow of high-purity argon.

Apparatus and measurement procedure

Heat capacity of $[(\eta^6\text{-}(m\text{-xylene}))_2\text{Mo}]^{\bullet+}[\text{C}_{60}]^{\bullet-}$ was measured over the range 8–320 K in a BKT-3.0 fully automatic adiabatic vacuum calorimeter with liquid helium and nitrogen used as cooling agents. The calorimeter design and measurement procedure are similar to those reported elsewhere [25–27]. The reliability of its operation was tested by measuring the heat capacity of special purity copper, standard synthetic corundum, and K-3 benzoic acid prepared at the D.I. Mendeleev All-Russian Institute for Metrology (VNIIM). It was established by the calibration that the determination of the heat capacity C_p° of substances was measured with an error not exceeding $\pm 2\%$ at $T = (8\text{--}15)$ K, $\pm 0.5\%$ between 15 and 40 K, and $\pm 0.2\%$ in the range from 40 to 320 K. The phase transition temperatures are measured within about ± 0.01 K and the enthalpies of transformations with the error of $\pm 0.2\%$.

The heat capacity of $[(\eta^6\text{-}(m\text{-xylene}))_2\text{Mo}]^{\bullet+}[\text{C}_{60}]^{\bullet-}$ was measured between 8 and 320 K with a sample mass of 0.2108 g. The pressure of the heat-exchange gas (high-purity helium) in the calorimeter was 40 kPa at room temperature. In the BKT-3.0 calorimeter, 182 experimental C_p° values were obtained in three series of experiments. The first series of measurements was completed in the temperature range from 8 to 80 K. The second series of C_p° measurements was carried out between $T = (79$ and 320) K. The sample was cooled down to $T = 174$ K and a repeated cycle of C_p° measurements (third series) was conducted to $T = 220$ K. In the whole temperature range under study the heat capacity of $[(\eta^6\text{-}(m\text{-xylene}))_2\text{Mo}]^{\bullet+}[\text{C}_{60}]^{\bullet-}$ was 15–30% of the total heat capacity of the calorimetric ampoule with the substance. The experimental C_p° values were smoothed by the fitting to exponential and semi-logarithmic polynomials. As an example, the polynomials with the corresponding coefficients for ranges from 118 to 175 K and from 220 to 320 K are cited below. For fulleride in the interval between 118 and 175 K, the equation $\ln C_p^\circ(T) = -256.3026 + 620.0907 \ln(T/30) - 359.1707 \cdot \{\ln(T/30)\}^2 - 247.1144 \cdot \{\ln(T/30)\}^3 + 389.8998 \cdot \{\ln(T/30)\}^4 - 170.2836 \cdot \{\ln(T/30)\}^5 + 25.7551 \cdot \{\ln(T/30)\}^6$ as well as the equation $\ln C_p^\circ(T) = 294.9528 - 1080.057 \cdot \ln(T/30) + 1548.7172 \cdot \{\ln(T/30)\}^2 - 1109.1598 \cdot \{\ln(T/30)\}^3 + 412.1933 \cdot \{\ln(T/30)\}^4 - 67.6072 \cdot \{\ln(T/30)\}^5 + 0.925413 \cdot \{\ln(T/30)\}^6$ in the range from 220 to 320 K were used.

In the above equations the C_p° is given in $\text{J K}^{-1} \text{mol}^{-1}$.

The mean-square deviation of the C_p° points from the smooth curve did not exceed $\pm 0.9\%$ in the range 8–20 K, $\pm 0.2\%$ between 20 and 320 K. The molar mass of the object under study was calculated from the IUPAC table of atomic weights [28].

Results and discussion

Heat capacity

Experimental values of heat capacity of $[(\eta^6\text{-}(m\text{-xylene}))_2\text{Mo}]^+[\text{C}_{60}]^{\bullet-}$ over the range from 8.55 to 320.6 K (Table 1) and the smoothed $C_p^\circ = f(T)$ plot are illustrated in Fig. 1. It can be seen that heat capacity of fulleride gradually increases with rising temperature until 175 K. In the temperature interval from 175 to 220 K, endothermic transformation occurs that manifest itself as a positive deviation from the normal trend of the temperature dependence of C_p° (Fig. 1).

The heat capacity grows relatively rapidly from $523.7 \text{ J K}^{-1} \text{mol}^{-1}$ at 175 K until the p. C (Fig. 1) and then it decreases down to $693 \text{ J K}^{-1} \text{mol}^{-1}$ at 220.7 K. The above temperature region for the relation $C_p^\circ = f(T)$ is described by the BCD curve. The transition is reversible. It was reproduced on repeated cooling and heating (as it described above). The transition enthalpy $\Delta_{\text{tr}}H_m^\circ = (4.82 \pm 0.05) \text{ kJ} \cdot \text{mol}^{-1}$ was determined graphically as an area bounded with BCDB (Fig. 1).

A similar transition was detected earlier for fullerides $[(\eta^6\text{-C}_7\text{H}_8)_2\text{Cr}]^+[\text{C}_{60}]^{\bullet-}$ [12] over the range from 245 to 265 K and for $[(\eta^6\text{-Ph}_2)_2\text{Cr}]^+[\text{C}_{60}]^{\bullet-}$ [16], $[(\eta^6\text{-}t\text{-BuPh})_2\text{Cr}]^+[\text{C}_{60}]^{\bullet-}$ [17] and $[(\eta^6\text{-EtOPh})_2\text{Cr}]^+[\text{C}_{60}]^{\bullet-}$ [18] in the range 270–320, 170–210 and 160–250 K, respectively, studied by us. The authors of Ref. [12] interpreted this transformation as the first-order equilibrium phase transition from a three-wedge low-temperature phase to a simple cubic high-temperature one on heating. It was shown [12, 14] that at $T > 265 \text{ K}$ the fulleride $[(\eta^6\text{-C}_7\text{H}_8)_2\text{Cr}]^+[\text{C}_{60}]^{\bullet-}$ existed in the form of a dynamically disordered anion of fullerene and *bis*-(η^6 -toluene)chromium cation while at $T < 245 \text{ K}$ the sample was in the form of ordered dimers $(\text{C}_{60}^-)_2$ with two cations of *bis*-(η^6 -toluene)chromium. The authors came to these conclusions based on the structural data on the bond lengths and angles in $[(\eta^6\text{-C}_7\text{H}_8)_2\text{Cr}]^+[\text{C}_{60}]^{\bullet-}$ molecules at different temperatures and thus, the inference about the low-temperature dimerization of fullerene fragments in the fulleride was made [12]. According to X-ray data [15], it was found that at room temperature *bis*-(η^6 -biphenyl)chromium fulleride $[(\eta^6\text{-Ph}_2)_2\text{Cr}]^+[\text{C}_{60}]^{\bullet-}$ is a monomer with a fairly ordered

Table 1 Experimental data of molar heat capacity of $[(\eta^6\text{-}(m\text{-xylene}))_2\text{Mo}]^+[\text{C}_{60}]^{\bullet-}$ in $\text{J mol}^{-1} \text{K}^{-1}$; $M = 1028.93 \text{ g mol}^{-1}$, $p^\circ = 0.1 \text{ MPa}$

| T/K | C_p° |
|-----------------|-------------|
| <i>Series 1</i> | |
| 8.55 | 11.4 |
| 8.79 | 12.4 |
| 8.84 | 12.7 |
| 9.04 | 13.4 |
| 9.25 | 14.1 |
| 9.38 | 14.3 |
| 9.62 | 15.1 |
| 9.88 | 16.1 |
| 10.09 | 17.4 |
| 10.37 | 18.6 |
| 10.74 | 19.8 |
| 11.14 | 21.3 |
| 11.53 | 23.2 |
| 11.93 | 24.2 |
| 12.36 | 25.6 |
| 12.78 | 27.0 |
| 13.22 | 28.4 |
| 13.68 | 30.0 |
| 14.13 | 31.7 |
| 14.59 | 33.4 |
| 15.06 | 35.5 |
| 15.55 | 37.3 |
| 16.10 | 38.80 |
| 16.98 | 41.79 |
| 17.34 | 43.00 |
| 17.62 | 43.77 |
| 18.14 | 45.70 |
| 18.66 | 47.58 |
| 19.20 | 49.70 |
| 19.77 | 51.70 |
| 20.93 | 55.90 |
| 22.41 | 61.20 |
| 23.90 | 65.90 |
| 25.41 | 70.50 |
| 26.93 | 74.70 |
| 28.46 | 79.30 |
| 30.01 | 83.17 |
| 31.57 | 86.71 |
| 33.14 | 91.54 |
| 34.73 | 95.81 |
| 36.32 | 99.80 |
| 37.93 | 102.4 |
| 39.54 | 106.1 |
| 41.17 | 110.1 |
| 42.79 | 113.4 |
| 44.43 | 116.6 |

Table 1 continued

| T/K | C_p^0 |
|-----------------|---------|
| 46.12 | 120.0 |
| 47.78 | 122.7 |
| 49.43 | 125.8 |
| 51.10 | 128.1 |
| 52.76 | 130.6 |
| 54.44 | 133.6 |
| 56.12 | 136.6 |
| 57.80 | 139.7 |
| 59.49 | 142.1 |
| 61.19 | 146.3 |
| 62.88 | 149.3 |
| 64.60 | 152.5 |
| 66.30 | 155.7 |
| 68.00 | 159.2 |
| 69.71 | 163.1 |
| 71.55 | 167.4 |
| 74.38 | 172.9 |
| 76.85 | 178.4 |
| 78.78 | 181.6 |
| 80.78 | 185.3 |
| <i>Series 2</i> | |
| 79.34 | 182.3 |
| 81.24 | 186.3 |
| 82.88 | 190.3 |
| 82.77 | 189.7 |
| 84.69 | 193.9 |
| 86.44 | 197.6 |
| 88.20 | 201.6 |
| 89.98 | 206.7 |
| 91.78 | 211.4 |
| 93.59 | 215.3 |
| 95.42 | 220.5 |
| 97.26 | 224.7 |
| 99.11 | 229.9 |
| 101.41 | 235.8 |
| 104.12 | 244.0 |
| 106.85 | 251.9 |
| 109.57 | 262.4 |
| 112.42 | 271.8 |
| 115.14 | 280.4 |
| 117.87 | 288.8 |
| 120.59 | 295.8 |
| 123.31 | 306.5 |
| 126.03 | 314.8 |
| 128.75 | 324.1 |
| 131.47 | 330.4 |
| 134.18 | 341.9 |
| 136.90 | 350.0 |

Table 1 continued

| T/K | C_p^0 |
|--------|---------|
| 139.62 | 360.1 |
| 142.34 | 368.2 |
| 145.05 | 382.0 |
| 147.77 | 390.7 |
| 150.48 | 402.2 |
| 153.20 | 415.0 |
| 156.02 | 427.5 |
| 158.74 | 437.7 |
| 161.45 | 447.7 |
| 164.16 | 461.6 |
| 166.86 | 478.1 |
| 169.57 | 490.7 |
| 172.28 | 508.8 |
| 174.99 | 523.7 |
| 177.69 | 541.0 |
| 180.39 | 557.2 |
| 183.07 | 572.9 |
| 187.05 | 621.0 |
| 190.85 | 660.3 |
| 193.54 | 715.3 |
| 196.22 | 801.1 |
| 198.87 | 1005 |
| 201.49 | 1317 |
| 204.23 | 729.2 |
| 207.00 | 694.3 |
| 209.71 | 684.6 |
| 212.43 | 683.3 |
| 215.13 | 686.8 |
| 216.78 | 688.0 |
| 219.00 | 685.0 |
| 220.70 | 693.0 |
| 222.05 | 696.0 |
| 224.72 | 705.7 |
| 227.40 | 715.7 |
| 230.06 | 724.0 |
| 232.73 | 731.4 |
| 235.40 | 741.6 |
| 238.07 | 750.4 |
| 240.74 | 758.2 |
| 243.40 | 768.6 |
| 246.06 | 777.9 |
| 248.72 | 787.1 |
| 251.37 | 797.5 |
| 254.07 | 807.0 |
| 256.71 | 815.1 |
| 259.33 | 825.2 |
| 261.95 | 835.0 |
| 264.55 | 842.7 |

Table 1 continued

| T/K | C_p^0 |
|-----------------|---------|
| 267.14 | 852.5 |
| 269.72 | 863.2 |
| 272.27 | 872.5 |
| 274.81 | 883.0 |
| 277.33 | 892.0 |
| 279.82 | 902.7 |
| 282.29 | 913.7 |
| 284.73 | 923.4 |
| 287.14 | 934.6 |
| 289.52 | 945.9 |
| 292.10 | 958.0 |
| 294.80 | 971.7 |
| 296.91 | 983.0 |
| 301.10 | 1005 |
| 305.30 | 1029 |
| 308.10 | 1045 |
| 310.60 | 1064 |
| 313.40 | 1082 |
| 316.00 | 1103 |
| 316.92 | 1108 |
| 317.84 | 1115 |
| 318.77 | 1122 |
| 319.67 | 1130 |
| 320.61 | 1136 |
| <i>Series 3</i> | |
| 174.85 | 515.5 |
| 178.27 | 538.7 |
| 182.08 | 550.4 |
| 184.77 | 585.7 |
| 187.46 | 609.3 |
| 190.13 | 642.2 |
| 192.81 | 689.5 |
| 195.47 | 763.6 |
| 198.11 | 923.2 |
| 200.71 | 1326 |
| 203.37 | 814.0 |
| 206.12 | 697.8 |
| 208.81 | 684.1 |
| 211.49 | 681.3 |
| 214.16 | 676.8 |
| 216.83 | 681.7 |
| 219.49 | 687.3 |
| 222.23 | 696.5 |

cation $[(\eta^6\text{-Ph}_2)_2\text{Cr}]^{\bullet+}$ and a disordered anion-radical of fullerene in the structure whereas in a lower-temperature range ($T = 100$ K) the anion-radicals $\text{C}_{60}^{\bullet-}$ in this compound are ordered into the dimers via a single link.

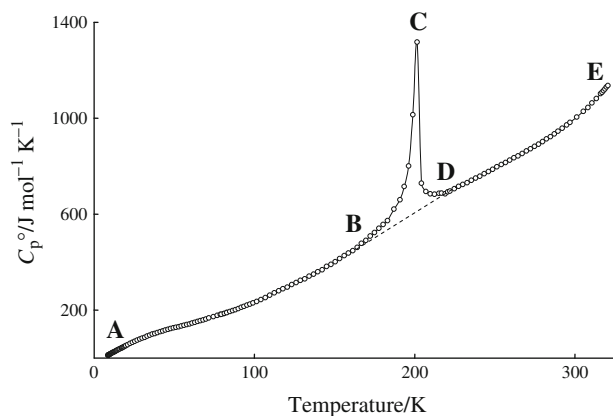


Fig. 1 Heat capacity of the bis-(η^6 -*m*-xylene)molybdenum fulleride: *AB* dimeric form, *DE* monomeric form, and *BCD* apparent heat capacity in the transformation interval

As opposed to the authors of Ref. [12], we [16–18] suggested to consider this transformation as superposition of the physical transition—the ordering of the structure on cooling—and the process of chemical nature, i.e., the association of anion-radicals of fullerene by means of the formation of a single link between them. We therefore believe that the thermodynamically equilibrium transition temperature and entropy cannot be determined using the equation of the second law of thermodynamics, as is usually done for first-order phase transitions [29].

For the sample tested in the present work, $[(\eta^6\text{-}(m\text{-xylene}))_2\text{Mo}]^{\bullet+}[\text{C}_{60}]^{\bullet-}$, the indicated endothermic transformation has the same nature as for fullerides $[(\eta^6\text{-C}_7\text{H}_8)_2\text{Cr}]^{\bullet+}[\text{C}_{60}]^{\bullet-}$ [12, 14], $[(\eta^6\text{-Ph}_2)_2\text{Cr}]^{\bullet+}[\text{C}_{60}]^{\bullet-}$ [16], $[(\eta^6\text{-}t\text{-BuPh})_2\text{Cr}]^{\bullet+}[\text{C}_{60}]^{\bullet-}$ [17] and $[(\eta^6\text{-EtOPh})_2\text{Cr}]^{\bullet+}[\text{C}_{60}]^{\bullet-}$ [18]. According to electron paramagnetic resonance data, the ESR spectrum of the solid sample $[(\eta^6\text{-}(m\text{-xylene}))_2\text{Mo}]^{\bullet+}[\text{C}_{60}]^{\bullet-}$ at 291 K (Fig. 2) is given by the symmetrical singlet and has the g -factor equal to 1.9921 ($\Delta H = 133$ G), which is intermediate between those characteristic of $[(\eta^6\text{-}(m\text{-xylene}))_2\text{Mo}]^{\bullet+}$ (1.988) and $\text{C}_{60}^{\bullet-}$ (1.9996–2.0000) [30] because of strong exchange coupling between $[(\eta^6\text{-}(m\text{-xylene}))_2\text{Mo}]^{\bullet+}$ and $\text{C}_{60}^{\bullet-}$. The ESR spectrum at 122 K (Fig. 2) is a single line with $g = 1.9879$ and $\Delta H = 53$ G, which is characteristic of non-interacting paramagnetic $[(\eta^6\text{-}(m\text{-xylene}))_2\text{Mo}]^{\bullet+}$. Such behavior is characteristic of $[(\eta^6\text{-C}_7\text{H}_8)_2\text{Cr}]^{\bullet+}[\text{C}_{60}]^{\bullet-}$ and $[(\eta^6\text{-C}_6\text{H}_6)_2\text{Cr}]^{\bullet+}[\text{C}_{60}]^{\bullet-}$ [20] and is related to dimerization of anion-radicals of fullerene on cooling. It should be noted that the value of ESR signal g -factor for fulleride $[(\eta^6\text{-}(m\text{-xylene}))_2\text{Mo}]^{\bullet+}[\text{C}_{60}]^{\bullet-}$ changes abruptly by in the range from 175 to 220 K (Fig. 3) under cooling. Such behavior points to dimerization of fullerene anion-radicals in $[(\eta^6\text{-}(m\text{-xylene}))_2\text{Mo}]^{\bullet+}[\text{C}_{60}]^{\bullet-}$ composition in this temperature interval. The temperature dependence of heat capacity $C_p^0 = f(T)$ (Fig. 1) characterizes the two different states: dimer $(\text{C}_{60}^{\bullet-})_2$ with two cations $[(\eta^6\text{-}(m\text{-xylene}))_2\text{Mo}]^{\bullet+}$ until 175 K and

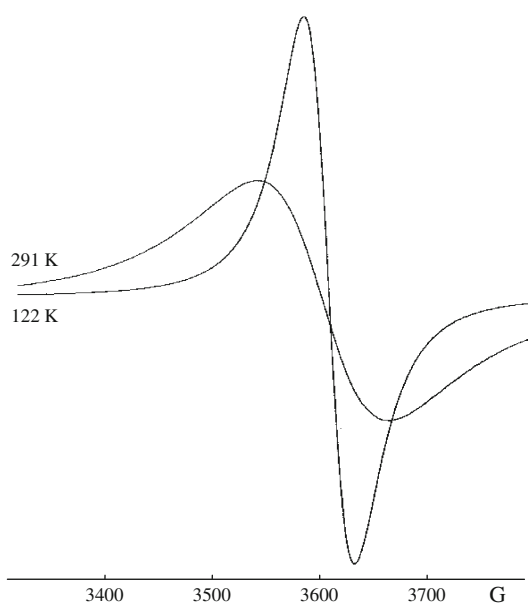


Fig. 2 EPR spectra of the crystalline $[(\eta^6\text{-}(m\text{-xylene}))_2\text{Mo}]^+[\text{C}_{60}]^-$ at different temperatures

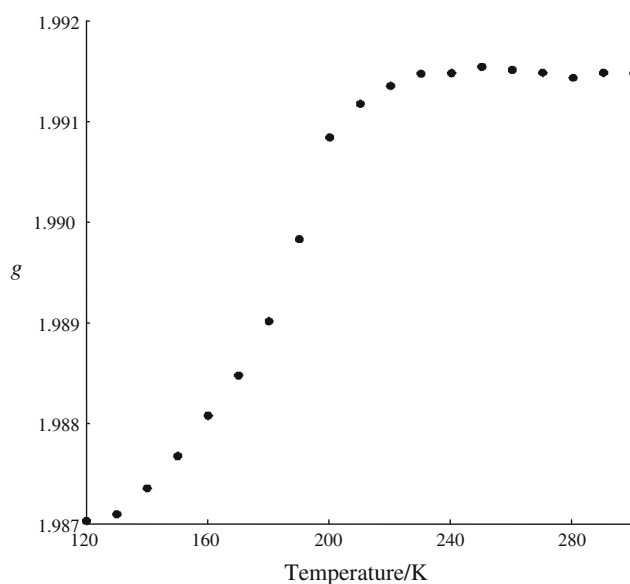


Fig. 3 The temperature dependence of g -factor in ESR signal of the crystalline $[(\eta^6\text{-}(m\text{-xylene}))_2\text{Mo}]^+[\text{C}_{60}]^-$

$[(\eta^6\text{-}(m\text{-xylene}))_2\text{Mo}]^+[\text{C}_{60}]^-$ after 220 K. In the range between 175 and 220 K it is a mixture of dimeric and monomeric forms of fulleride.

A comparison of the temperature intervals of the dissociation of the $(\text{C}_{60}^-)_2$ dimers formed in the $[(\eta^6\text{-}(m\text{-xylene}))_2\text{Mo}]^+[\text{C}_{60}]^-$ and some fullerides [16–18], and the decomposition of the $(\text{C}_{60})_2$ neutral dimer to fullerite C_{60} [24] reveals certain peculiarities. The dissociation of the $(\text{C}_{60}^-)_2$ dimer takes place at a noticeably lower

temperature and the process occurs in a much narrower temperature interval and reversibly. For instance, the decomposition of the $(\text{C}_{60})_2$ neutral dimer to fullerite C_{60} occurs at 380–490 K [24], whereas the dissociation of the $(\text{C}_{60}^-)_2$ dimer formed in the system under consideration, at 175–220 K. These differences are caused by the nature of binding of fullerene fragments in compounds. In the $(\text{C}_{60})_2$ neutral dimer [24], C_{60} molecules are bound by rigid covalent bonds according to the [2 + 2] cycloaddition mechanism. In fullerides, the low-temperature dimerization of C_{60} fragments with the formation of $(\text{C}_{60}^-)_2$ dimeric dianions occurs with the formation of single bonds. It should be also noted that for the fulleride being considered in this article, the dissociation of the $(\text{C}_{60}^-)_2$ under at heating begins at the lowest temperature ($T = 175$ K) for $[(\eta^6\text{-}(m\text{-xylene}))_2\text{Mo}]^+[\text{C}_{60}]^-$, which is indicative of its relatively lower thermal stability. Thus, the stability of dimeric dianions $(\text{C}_{60}^-)_2$ depends significantly on the nature of substituent.

For the fulleride under study the G -type transition and orientation phase transition [30–33] known for fullerite C_{60} are absent on the $C_p^\circ = f(T)$ curve (Fig. 1), which testifies to the fully bonded fullerene fragments in the complex.

The temperature dependence of heat capacity $C_p^\circ = f(T)$ in the low-temperature region ($T < 20$ K) is well described by the limiting law $C_p^\circ = AT^3$ for the tested fulleride $[(\eta^6\text{-}(m\text{-xylene}))_2\text{Mo}]^+[\text{C}_{60}]^-$ as well as for fullerite C_{60} [33], neutral dimer $(\text{C}_{60})_2$ [24] and fullerides $[(\eta^6\text{-Ph}_2)_2\text{Cr}]^+[\text{C}_{60}]^-$ [16], $[(\eta^6\text{-}i\text{-BuPh})_2\text{Cr}]^+[\text{C}_{60}]^-$ [17] and $[(\eta^6\text{-EtOPh})_2\text{Cr}]^+[\text{C}_{60}]^-$ [18] which is characteristic of the solids of Debye's nature.

Standard thermodynamic functions

The standard thermodynamic functions of the crystalline fulleride dimer (Table 2) were calculated from the C_p° values in the range $T \rightarrow (0\text{--}175)$ K and for the monomeric complex $[(\eta^6\text{-}(m\text{-xylene}))_2\text{Mo}]^+[\text{C}_{60}]^-$ —in the range from 220 to 320 K (Table 3). The C_p° data over the range $T \rightarrow (0\text{--}8)$ K were determined by the extrapolation of the $C_p^\circ = f(T)$ curve from the Debye function of solids:

$$C_p^\circ = nD(\theta_D/T), \quad (1)$$

where D denotes Debye function, $n = 9$ and $\theta_D = 65.0$ K are specially selected parameters. With such parameters, Eq. 1 describes the experimental C_p° values of the compound in the range from 8 to 13 K with the error $\pm 1.5\%$. It was assumed that from 0 to 8 K, Eq. 1 reproduces the C_p° values with the same error.

The calculations of enthalpy $H^\circ(T_2) - H^\circ(T_1)$ and entropy $S^\circ(T_2) - S^\circ(T_1)$ were made by the numerical integration of $C_p^\circ = f(T)$ and $C_p^\circ = \ln f(T)$ curves, respectively. The Gibbs function $G^\circ(T_2) - G^\circ(T_1)$ was calculated with

Table 2 Standard thermodynamic functions of the dimeric bis-(η^6 -m-xylene)molybdenum fulleride $[(\eta^6\text{-}(m\text{-xylene}))_2\text{Mo}]^{*+}[\text{C}_{60}]^{*-}$; $M = 1028.93 \text{ g mol}^{-1}$

| T/K | $C_p^0/\text{J mol}^{-1} \text{ K}^{-1}$ | $H^\circ(T)-H^\circ(0)/\text{kJ mol}^{-1}$ | $S^\circ(T)/\text{J mol}^{-1} \text{ K}^{-1}$ | $-[G^\circ(T)-H^\circ(0)]/\text{kJ mol}^{-1}$ |
|--------------|--|--|---|---|
| 5 | 2.67 | 0.00300 | 0.894 | 0.00100 |
| 10 | 17.0 | 0.0480 | 6.50 | 0.0170 |
| 15 | 35.1 | 0.179 | 16.9 | 0.0740 |
| 20 | 52.52 | 0.3975 | 29.34 | 0.1894 |
| 25 | 69.37 | 0.7037 | 42.94 | 0.3698 |
| 30 | 83.02 | 1.086 | 56.82 | 0.6192 |
| 35 | 96.41 | 1.534 | 70.62 | 0.9379 |
| 40 | 107.2 | 2.043 | 84.21 | 1.325 |
| 45 | 118.0 | 2.607 | 97.47 | 1.780 |
| 50 | 126.4 | 3.218 | 110.4 | 2.299 |
| 60 | 143.6 | 4.565 | 134.9 | 3.526 |
| 70 | 163.6 | 6.101 | 158.5 | 4.994 |
| 80 | 184.0 | 7.838 | 181.7 | 6.695 |
| 90 | 206.4 | 9.789 | 204.6 | 8.626 |
| 100 | 232.1 | 11.98 | 227.6 | 10.79 |
| 110 | 263.3 | 14.45 | 251.2 | 13.18 |
| 120 | 294.5 | 17.25 | 275.5 | 15.81 |
| 130 | 325.8 | 20.35 | 300.3 | 18.69 |
| 140 | 360.7 | 23.78 | 325.7 | 21.82 |
| 150 | 400.2 | 27.58 | 351.9 | 25.21 |
| 160 | 443.4 | 31.79 | 379.1 | 28.86 |
| 170 | 493.1 | 36.47 | 407.4 | 32.79 |
| 175 | 516.9 | 38.49 | 419.2 | 34.45 |

Table 3 Standard thermodynamic functions of the monomeric bis-(η^6 -m-xylene)molybdenum fulleride $[(\eta^6\text{-}(m\text{-xylene}))_2\text{Mo}]^{*+}[\text{C}_{60}]^{*-}$; $M = 1028.93 \text{ g mol}^{-1}$

| T/K | $C_p^0/\text{J mol}^{-1} \text{ K}^{-1}$ | $H^\circ(T)-H^\circ(220)/\text{kJ mol}^{-1}$ | $S^\circ(T)-S^\circ(220)/\text{J mol}^{-1} \text{ K}^{-1}$ | $-G^\circ(T)-G^\circ(220)]/\text{kJ mol}^{-1}$ |
|--------------|--|--|--|--|
| 220 | 689.4 | 0 | 0 | 0 |
| 230 | 723.4 | 7.071 | 31.40 | 0.1506 |
| 240 | 757.2 | 14.47 | 62.90 | 0.6283 |
| 250 | 791.6 | 22.22 | 94.51 | 1.409 |
| 260 | 826.9 | 30.30 | 126.2 | 2.519 |
| 270 | 864.0 | 38.76 | 158.1 | 3.934 |
| 280 | 903.9 | 47.59 | 190.3 | 5.682 |
| 290 | 948.0 | 56.86 | 222.7 | 7.740 |
| 298.15 | 988.7 | 64.75 | 249.6 | 9.665 |
| 300 | 998.7 | 66.57 | 255.7 | 10.14 |
| 310 | 1059 | 76.86 | 289.4 | 12.86 |
| 320 | 1132 | 87.79 | 324.1 | 15.93 |

Gibbs–Helmholtz equation from $H^\circ(T_2)-H^\circ(T_1)$ and $S^\circ(T_2)-S^\circ(T_1)$ values at corresponding temperatures. The calculation procedure was described in detail in Refs. [34, 35].

The determined errors of the function values are $\pm 2\%$ at $T < 15 \text{ K}$, $\pm 0.5\%$ from 15 to 40 K, and $\pm 0.2\%$ in the range between 40 and 320 K.

Conclusions

- The heat capacity of crystalline *bis*-(η^6 -*m*-xylene) molybdenum fulleride has been measured over the range from 8 to 320 K.
- In the range 175–220 the reversible transformation was observed during heating; it was caused by the dissociation of the $(C_{60}^-)_2$ dimer and the formation of the $[(\eta^6$ -*m*-xylene) $)_2Mo]^{*+}[C_{60}]^{*-}$ fulleride. The temperature dependence of EPR signal parameters of *bis*-(η^6 -*m*-xylene)molybdenum fulleride in the range from 120 to 300 K was investigated by electron paramagnetic resonance. The standard thermodynamic characteristics of the transformation were determined.
- From experimental data the standard thermodynamic functions of $[(\eta^6$ -*m*-xylene) $)_2Mo]^{*+}[C_{60}]^{*-}$ have been calculated for dimeric fulleride in the interval from $T \rightarrow 0$ to 175 K as well as for monomeric $[(\eta^6$ -*m*-xylene) $)_2Mo]^{*+}[C_{60}]^{*-}$ complex between 220 and 320 K.
- The comparison of thermodynamic properties of fulleride under study and initial C_{60} fullerite, neutral dimer $(C_{60})_2$ as some fulleride studied earlier was made.

Acknowledgements This study was performed with the financial support of the Russian Foundation of Basic Research (Projects No. 08-03-00214a, 09-03-97034-p-povol-a, 09-03-97045-p-povol-a, and 10-03-00968a), and the Ministry of Science and Education (Contract No P-337).

References

1. Kratschmer W, Lamb LD, Fostiropoulos K, Huffman DR. Solid C_{60} : a new form of carbon. *Nature*. 1990;347:354–8.
2. Konarev DN, Lyubovskaya RN. Donor–acceptor complexes and radical ionic salts based on fullerenes. *Rus Chem Rev*. 1999;68:19–38.
3. Stankevich IV, Sokolov VI. Advances in fullerene chemistry. *Rus Chem Bull*. 2004;9:1824–45.
4. Karaulova EN, Bagrii EI. Fullerenes: functionalization and prospects for the use of derivatives. *Rus Chem Rev*. 1999;68:889–907.
5. Kowalska E, Czerwos E, Kozłowski M, Surga W, Radomska J. Structural, thermal, and electrical properties of carbonaceous films containing palladium nanocrystals. *J Thermal Anal Calorim*. 2010;101:737–42.
6. Konarev DV, Khasanov SS, Saito G, Lyubovskaya RN. Design of molecular and ionic complexes of fullerene C_{60} with metal(II) octaethylporphyrins, M^II OEP ($M = Zn, Co, Fe, \text{ and } Mn$) containing coordination M–N(ligand) and M–C(C_{60}^-) bonds. *Cryst Growth Des*. 2009;9:1170–81.
7. Konarev DV, Kovalevsky AYU, Otsuka A, Saito G, Lyubovskaya RN. Neutral and ionic complexes of C_{60} with metal dibenzylidithiocarbamates. Reversible dimerization of C_{60}^{*-} in ionic multicomponent complex $[Cr(C_6H_6)_2]^{*+}(C_{60}^{*-})_2 \cdot 0.5[Pd(dbtc)_2]$. *Inorg Chem*. 2005;44:9547–53.
8. Konarev DV, Khasanov SS, Saito G, Otsuka A, Lyubovskaya RN. Ionic and neutral C_{60} complexes with coordination assemblies of metal tetraphenylporphyrins, M^II TPP $_2$ ·DMP ($M = Mn, Zn$). Coexistence of $(C_{60}^-)_2$ dimers bonded by one and two single bonds in the same compound. *Inorg Chem*. 2007;46:7601–9.
9. Konarev DV, Khasanov SS, Saito G, Vorontsov II, Otsuka A, Lyubovskaya RN, Antipin YuM. Crystal structure and magnetic properties of an ionic C_{60} complex with decamethylcobaltocene: $(Cp_2Co)_2C_{60}(C_6H_4Cl_2, C_6H_5CN)_2$. Singlet-triplet transitions in the C_{60}^{2-} anion. *Inorg Chem*. 2003;42:3706–8.
10. Konarev DV, Khasanov SS, Kovalevsky AYU, Lopatin DV, Rodaev VV, Saito G, Náfrádi B, Forró L, Lyubovskaya RN. Supramolecular approach to the synthesis of [60]Fullerene-Metal dithiocarbamate complexes, $(MII(R_2dtc)_2)_x \cdot L \cdot C_{60}$ ($M = Zn, Cd, Hg, Fe, \text{ and } Mn; x = 1 \text{ and } 2$). The study of magnetic properties and photoconductivity. *Cryst Growth Des*. 2008;8:1161–72.
11. Domrachev GA, Shevelev YuA, Cherkasov VK, Markin GV, Horshev SYa, Makarenko NP, Kaverin BS. Synthesis, property and thermodecomposition of bis-arene-chromium fullerides. In Proceedings of VI Int. Workshop on Fullerenes and Atomic Clusters, St. Petersburg, 2003, 151 (in Russian).
12. Honnerscheid A, Dinnebier R, Jansen M. Reversible dimerization of C_{60} molecules in the crystal structure of the *bis*(arene)chromium fulleride $[Cr(C_7H_8)]_2C_{60}$. *Acta Cryst*. 2002;858:482–8.
13. Domrachev GA, Shevelev YuA, Cherkasov VK, Fukin GK, Horshev SYa, Markin GV, Kaverin BS. Synthesis, structure, and thermodecomposition of *bis*(arene)chromium(I) fullerides. *Doel Chem*. 2004;395:74–7.
14. Honnerscheid A, Wullen L, Jansen M, Rahmer J, Mehring M. Dimer-formation in the *bis*(arene)chromium fulleride $Cr(C_7H_8)_2C_{60}$. *J Chem Phys*. 2001;115:7161–5.
15. Domrachev GA, Shevelev YuA, Cherkasov VK, Markin GV, Fukin GK, Horshev SYa, Kaverin BS, Karnatchevich VL. Formation, properties, and thermal decomposition of *bis*arene chromium (I) and molybdenum (I) fullerides. *Russ Chem Bull*. 2004;53:1–4.
16. Smirnova NN, Markin AV, Bykova TA, Boronina IE, Domrachev GA, Shevelev YuA, Markin GV. Thermodynamics of *bis*-(η^6 -diphenyl)chromium (I) fulleride $[(\eta^6$ -Ph) $)_2Cr]^{*+}[C_{60}]^{*-}$ in the range from $T \rightarrow (0 \text{ to } 360)$ K. *J Chem Thermodyn*. 2006;38:810–6.
17. Ruchenin VA, Markin AV, Smirnova NN, Markin GV, Shevelev YuA, Cherkasov VK, Kuropatov VA, Ketkov SYu, Lopatin MA, Domrachev GA. Thermodynamics of the *bis*-(η^6 -*t*-butylphenyl)chromium fulleride $[Cr\{\eta^6$ -(*t*-BuPh) $}_2\}^{*+}C_{60}^{*-}$. *Bull Chem Soc Jpn*. 2009;82:65–9.
18. Ruchenin VA, Markin AV, Smirnova NN, Markin GV, Shevelev YuA, Kuropatov VA, Lopatin MA, Domrachev GA. The thermodynamic properties of *bis*(η^6 -ethoxybenzene)chromium fulleride from $T \rightarrow 0$ to 340 K. *Russ J Phys Chem A*. 2010;84:928–33.
19. Konarev DV, Khasanov SS, Saito G, Otsuka A, Yoshida Y, Lyubovskaya RN. Formation of single-bonded $(C_{60}^-)_2$ and $(C_{70}^-)_2$ dimers in crystalline ionic complexes of fullerenes. *J Am Chem Soc*. 2003;125:10074–83.
20. Konarev DV, Khasanov SS, AYU Kovalevsky, Saito G, Otsuka A, Lyubovskaya RN. Structural aspects of two-stage dimerization in an ionic C_{60} complex with *bis*(benzene)chromium: $Cr(C_6H_6)_2 \cdot C_{60} \cdot C_6H_4Cl_2$. *Dalton Trans*. 2006;30:3716–20.
21. Oszlanyi G, Bortel G, Faigel G, Granasy L, Stephens GM, Forro PW. Single C–C bond in $(C_{60})_2^{2-}$. *Rhys Rev*. 1996;54:11849–52.
22. Wang W, Komatsu K, Murata Y, Shiro M. Synthesis and X-ray structure of dumb-bell-shaped C_{120} . *Nature*. 1997;387:583–6.
23. Iwasa Y, Arima T, Fleming RM, Siegrist T, Zhou O, Haddon RC, Rothberg LJ, Lyons KB, Carter HL Jr, Hebard AF, Tyccko R, Dabbagh G, Krajewski JJ, Thomas GA, Yagi T. New phases of C_{60} synthesized at high pressure. *Science*. 1994;264:1570–2.

24. Markin AV, Lebedev BV, Smirnova NN, Davydov VA, Rakhmanina AV. Calorimetric study of crystalline dimer and polymerized phases of C₆₀ fullerene. *Thermochim Acta*. 2004; 421:73–80.
25. Varushchenko RM, Druzhinina AI, Sorkin EL. Low temperature heat capacity of 1-bromoperfluorooctane. *J Chem Thermodyn*. 1997;29:623–37.
26. Paukov IE, Kovalevskaya YA, Kiseleva IA, Shuriga TN. A low-temperature heat capacity study of natural lithium micas. *J Thermal Anal Calorim*. 2010;99:709–12.
27. Gatta GD, Richardson MJ, Sarge SM, Stolen S. Standards, calibration, and guidelines in microcalorimetry. part 2. Calibration standards for differential calorimetry. *Pure Appl Chem*. 2006;78: 1455–76.
28. Coplen TB. Atomic weights of the elements 1999 (IUPAC Technical Report). *Pure Appl Chem*. 2001;73:667–83.
29. Atkins PW. *Physical chemistry*. UK: Oxford University Press; 1978. p. 580.
30. Reed CA, Bolskar RD. Discrete fulleride anions and fullerenium cations. *Chem Rev*. 2000;100:1075–120.
31. Heiney PA, Fisher JE, McChie AR, Romanow WJ, Denenstein AM, McCauley JP Jr, Smith AB, Cox DE. Orientational ordering transition in solid C₆₀. *Phys Rev Lett*. 1991;66:2911–4.
32. Dworkin A, Szwarc H, Leach S, Hare JP, Dennis TJ, Kroto HW, Taylor R, Walton DRM. Thermodynamic evidence for a phase transition in crystalline fullerene C₆₀. *CR Acad Sci Paris Ser II*. 1991;312:979–82.
33. Lebedev BV, Zhogova KB, Bykova TA, Kaverin VS, Karnatsevich VL, Lopatin MA. Thermodynamics of C₆₀ fullerene in the 0–340 K range. *Rus Chem Bull*. 1996;45:2113–7.
34. McCullough JP, Scott DW. *Calorimetry of non-reacting systems*. London: Butterworth; 1968.
35. Lebedev BV. Application of precise calorimetry in study of polymers and polymerization processes. *Thermochim Acta*. 1997;297: 143–9.